

Annona atemoya leaf extract ameliorates cognitive impairment in amyloid- β injected Alzheimer's disease-like mouse model

Hye-Sun Lim¹, Yu Jin Kim^{1,2}, Eunjin Sohn¹, Jiyeon Yoon¹, Bu-Yeo Kim¹ and Soo-Jin Jeong¹ 

¹Clinical Medicine Division, Korea Institute of Oriental Medicine, Daejeon 34054, South Korea; ²College of Pharmacy, Chungnam National University, Daejeon 34134, South Korea

Corresponding author: Soo-Jin Jeong. Email: sjjeong@kiom.re.kr

Impact statement

Our study was aimed to find a novel candidate drug for Alzheimer's disease (AD) using natural products. We assessed the effects of *Annona atemoya* extracts on crucial events in the pathogenesis of AD. *A. atemoya* leaf (AAL) extract significantly inhibited amyloid- β aggregation, oxidative stress, neuronal cell death, and memory impairment through the epidermal growth factor receptor/G protein-coupled receptor kinase 2 pathway. Simultaneous analysis using HPLC determined six standard compounds of AAL extract, and rutin was identified as a bioactive compound. Of note, the anti-AD activity of AAL extract was more significant compared to other extracts from medicinal plants of which efficacy was previously reported. The potential of AAL extract as an anti-AD agent may provide insight into the new drug development for AD treatment.

Abstract

Annona atemoya is a hybrid of *Annona squamosa* and *Annona cherimola* that grow in several subtropical or tropical areas such as Florida in the US, Philippines, Cuba, Jamaica, Taiwan, and Jeju in South Korea. We report that the *A. atemoya* leaves (AAL) have inhibitory effects on the pathogenesis and regulatory mechanisms of Alzheimer's disease (AD). Ethanol extract of AAL prevented amyloid- β ($A\beta$) aggregation and increased free radical scavenging activity. In addition, AAL extract exerted protective effects against neuronal cell death in HT22 hippocampal cells. Moreover, oral administration of AAL extract significantly improved memory loss in the passive avoidance task and Y-maze test, as well as downregulated the expression of neuronal markers neuronal nuclei and brain-derived neurotrophic factor in $A\beta$ -injected AD mice. To verify the molecular mechanisms responsible for anti-AD actions of AAL, we conducted the antibody microarray analysis and found that epidermal growth factor receptor/G protein-coupled receptor kinase 2 signaling was activated in neuronal cells and AD-like mouse models. Additionally, quantitative analyses of the six standard compounds using high-performance liquid chromatography revealed that rutin is the most abundant compound of AAL. Furthermore, efficacy analyses of six standard

compounds showed that rutin and isoquercitrin had significant inhibitory activity on $A\beta$ aggregation. Taken together with biological activity and the content of compounds, rutin maybe a bioactive compound of AAL in the AD pathogenesis. Overall, our findings provide the first scientific support for the therapeutic effects of AAL in AD and AD-related disorders.

Keywords: *Annona atemoya*, amyloid- β , neuroprotection, memory improvement, Alzheimer's disease

Experimental Biology and Medicine 2019; 244: 1665–1679. DOI: 10.1177/1535370219886269

Introduction

Alzheimer's disease (AD) is a progressive neurodegenerative disease characterized by cognitive disruption. AD is considered life-threatening; yet, no cures for this disease exist. Currently, there are five medications approved by the US FDA for AD: tacrine, rivastigmine, galantamine, donepezil, and memantine. These drugs are sufficient to offer symptom relief¹ but have side effects such as diarrhea, nausea, muscle cramps, vomiting, fatigue, lowered blood pressure, insomnia, and loss of appetite.² Molecular targets of the approved medications are acetylcholinesterase

(AChE) or *N*-methyl-D-aspartate (NMDA) receptors. However, the limitations of AChE- or NMDA receptor-targeting drugs are becoming evident as they lack the ability to cure AD.

Amyloid- β ($A\beta$) is a crucial mediator in AD and is considered an attractive target molecule for developing novel AD medications. According to the amyloid hypothesis, the overproduction or accumulation of $A\beta$ in extracellular senile plaques occurs early in disease and is a central event in AD progression. Thus, controlling the production or accumulation of $A\beta$ plaques could be an effective

treatment and help to prevent AD. The amyloid hypothesis is regarded by many as a central description for AD progression, although recent failures of anti-A β drugs in clinical trials have been reported.^{3,4} Actually, the neuropathogenesis of AD caused by abnormal A β deposition is primarily initiated and occurred by oxidative stress.⁵ Thus, we investigated to find novel AD drug candidate(s) targeting A β with robust antioxidant activity.

Annona atemoya, also known as atemoya, is a hybrid between *A. squamosa* (sugar apple) and *A. cherimola* (cherimoya) that was first crossed by Wester in 1908, a horticulturist at the USDA's Subtropical Laboratory in Miami. *A. atemoya* is distributed in the subtropics and tropics such as Florida in the US, Philippines, Cuba, Jamaica, Taiwan, and Jeju in South Korea. *A. atemoya* fruit (AAF) is heart-shaped or round with pale-green and bumpy skin. It is used as an ingredient in juices, desserts, ice creams, or in natura.⁶⁻⁸ Bullatacin, an acetogenin isolated from AAF, has been reported to have anti-cancer activity in hepatoma cells.^{9,10} *A. atemoya* seed (AAS) was recently reported to have anti-angiogenic properties.¹¹ However, there are no reports on the biological activity of *A. atemoya* leaves (AAL). In the present study, we demonstrate that AAL extract possess anti-AD effects, and we demonstrate its molecular mechanisms using *in vitro* and *in vivo* experimental models. In addition, we established the simultaneous analysis methods of six standard compounds for quality control and identified the bioactive compound from AAL extract.

Materials and methods

Preparation of ethanol extract from *A. atemoya*, *Ginkgo biloba* (GB), *Lycium chinense* (LC), and *Angelica gigas* (AG)

A. atemoya was supported by Jeju Sunny Farm (Jeju, South Korea). The materials (AAL, AAF, and AAS) were dried and 2.7 kg of each was extracted twice with ethyl alcohol (60 L) for 3 h using the COSMOS-660 electric extractor (Kyungseo Machine Co., Incheon, South Korea). The extracted solutions were filtered, evaporated, and freeze-dried for making powdered extracts. GB, LC, and AG were obtained from the Naemome Dah (Ulsan, South Korea). Each material was dried and 50 g of each was extracted twice with ethyl alcohol (0.3 L) by refluxing for 2 h. The extracts were filtered and evaporated using a rotary evaporator.

Solvent fractionation of AAL

The powdered AAL extract (10 g) was suspended in H₂O (0.2 L) and in turn partitioned with *n*-hexane (HX), ethyl acetate (EA), and *n*-butanol (BU) to give extracts of 0.413 (4.13%), 0.424 (4.24%), and 1.373 g (13.73%), respectively (Figure 3(a)).

A β aggregation assay

A β aggregation assay was performed using SensoLyte[®] Thioflavin T β -Amyloid aggregation kit (AnaSpec,

Fremont, CA). A β ₁₋₄₂ peptides were stored at -80°C and used at 100 μ g/mL for the assay. Thioflavin T dye was prepared by dissolving in the Assay buffer included in the kit. AAL extract was dissolved in the Assay buffer (100 μ g/mL of final concentration). Thioflavin T (85 μ L) and AAL sample solution (5 μ L) were mixed and incubated in 96-well black microplate at 37°C. Fluorescence readings were expressed as the relative fluorescence units. All assays were completed in triplicates. The inhibition rate (%) of A β aggregation was assessed as described previously.¹²

Free radical scavenging activity

The free radical scavenging activity of ABTS and DPPH was used in the modified protocol of Re *et al.*¹³ and Moreno *et al.*,¹⁴ respectively. The absorbance of control or tested samples was assessed at 734 and 517 nm, respectively, and the activity for radical scavenging was calculated using the following equation

$$\text{Radical scavenging activity (\%)} = 1 - \frac{\text{Absorbance of tested sample}}{\text{Absorbance of control}} \times 100$$

Cell lines, maintenance and treatment

Murine hippocampal cell line HT22 were cultured in Dulbecco's modified Eagle's medium (Hyclone/Thermo, Rockford, IL), containing 10% fetal bovine serum (Hyclone/Thermo) and antibiotics penicillin/streptomycin at 37°C in a 5% CO₂ atmosphere. HT22 cells were concurrently treated with AAL, AAF, or AAS, and hydrogen peroxide (H₂O₂, 250 μ mol/L, Sigma-Aldrich, St Louis, MO) for 6 h.

Cell viability test

The cytotoxic effects of AAL, AAS, and AAF extracts were evaluated using CCK-8 assay kit (Dojindo Molecular Technology, Kumamoto, Japan). HT22 cells were seeded onto the 96 well micro-culture plates (3 \times 10⁴/well) and treated with AAL, AAS, or AAF extracts for 24 h and incubated with CCK solution for additional 4 h. Cell viability was determined using Epoch Microplate Spectrophotometer (BioTek Instruments, Inc., Winooski, VT)

$$\text{Cell viability (\%)} = \frac{\text{Absorbance at 450 nm in AAL, AAS or AAF - treated cells}}{\text{Absorbance at 450 nm in untreated cells}} \times 100$$

Brain-derived neurotrophic factor (BDNF) ELISA

An ELISA kit for BDNF was commercially obtained from R&D Systems (Minneapolis, MN). The culture supernatant was collected and applied to each well containing anti-BDNF. The amount of BDNF of each sample was determined using a BDNF standard curve.

Phospho-specific protein microarray analysis

Antibody array was performed using Full Moon Biosystem's Phospho Explorer Antibody Array kit (Sunnyvale, CA). Data normalization was conducted using the Genewiz 4.0 (Ocimum Biosolutions, Gaithersburg, MD) and determined the average intensity of samples comparable to that of all genes. For statistical analysis, MeV software ver. 4.9.0 (TM4 Development Group, Rockville, MD) was used for one-sample *t* tests. UniProt DB was used for annotation of the protein data and the phosphorylation ratio was determined as described previously.¹⁵

Western blotting

HT22 cell lysates were prepared using CelLytic™ MT Cell Lysis Reagent (Sigma-Aldrich). Tissues from mouse hippocampus were lysed in lysis buffer containing 1% Triton X-100, 1% deoxycholate, 0.1% sodium azide (Sigma-Aldrich), and protease inhibitors (Roche Diagnostics, Mannheim, Germany). Lysates were separated by sodium dodecyl sulfate-polyacrylamide gel electrophoresis using the 4–20% Mini-PROTEAN TGX Precast gels (Bio-Rad, Hercules, CA) and transferred to polyvinylidene fluoride membranes. For blocking the membranes, 5% skim milk in Tris-buffered saline containing Tween 20 (TBST) was used. The membranes were let an overnight incubation at 4°C with the desired primary antibodies for anti-phospho-Ca²⁺/calmodulin-dependent protein kinase II (CaMK2) $\beta/\nu/\delta$, phospho-epidermal growth factor receptor (EGFR), phospho-G protein-coupled receptor kinase 2 (GRK2), phospho-Myc, phospho-ferric reductase (FER), phospho-caveolin-1, phospho-nuclear factor kappa B (NF κ B) p65, phospho-myosin regulatory light chain (MLRN) 2 (Cell Signaling Technology, Beverly, MA), and glyceraldehyde 3-phosphate dehydrogenase (GAPDH; Santa Cruz Biotechnology, Santa Cruz, CA). After washing the membranes with TBST, they were incubated with anti-mouse or rabbit secondary antibody conjugated with horseradish peroxidase (Jackson Immuno Research, West Grove, PA) at room temperature for 1 h. After washing the membranes with TBST, they were developed using the Pierce ECL Western Blotting Substrate (Thermo Scientific, Rockford, IL).

Animals

Eight-week-old imprinting control region (ICR) male mice were obtained from Dae Han Bio Link (Eumseong, South Korea). Mice were bred in environmentally managed specific pathogen-free area at 22°C with light and dark cycling (12 h each) with providing water and standard food pellets ad libitum. Mice were grouped into five ($n=7$ /group): normal control, A β only, A β +AAL extract (50 or 100 mg/kg/day), and A β +morin (10 mg/kg/day). All animal experiments were carried out according to the National Institutes of Health Guidelines for the Care Use of Laboratory Animals. In addition, all assays were approved by the Institutional Animal Care and Use Committee of the Korea Institute of Oriental Medicine (Approval number: #17-034). Animal handling was

conducted according to the dictates of the National Animal Welfare Law of Korea.

Intracerebroventricular (icv) injection of A β ₁₋₄₂ aggregates

A β ₁₋₄₂ peptide (AnaSpec) was dissolved in PBS to 1 mM concentration and incubated at 37°C for five days to form A β aggregates. A β (10 μ mol/mouse) was infused (coordinates from bregma: anteroposterior = -0.5 mm, mediolateral = 1 mm, and dorsoventral = 2.5 mm) based on the brain in stereotaxic coordinates. A Hamilton syringe (26-gauge stainless-steel needle) was used to deliver A β aggregates (3 μ L/mouse) at a rate of 1 μ L/min into the icv region. Body temperature was maintained at 36.5 \pm 0.5°C. Normal control group was treated by the same procedure, except that the same volume of PBS was injected instead.

Passive avoidance test

A test box with two of equally sized chambers (40 \times 20 \times 30 cm³) divided by a guillotine door (5 \times 5 cm²); one part was lit with a 60-W bulb and the other part was dark. Floor in the dark box was composed of several stainless steel rods (5 mm) set 1 cm apart. All mice were daily fed either vehicle or AAL extract for 23 days. Two weeks after A β administration, each mouse was placed into the light side and allocated to travel for training, and the guillotine door was opened to allow the mice to move to the dark area. The same processes with above described were repeated next day with an electric foot shock (0.5 mA) for 3 s for immediately delivering to a mouse via the grid floor after moving the dark side. Latency time to the dark was recorded up to 300 s.

Y-maze test

The Y-maze test was conducted at day 18 after A β injection. Y-maze was composed of three black colored wood arms (40 long \times 12 high \times 3 wide cm³ at the bottom, and 10 cm wide at the top). The arms converged at a symmetrical triangular central point. A mouse was allowed to place at one arm and allocated to freely travel through the maze for 8 min. Percent of the alternation behavior was determined as a successive entry into each arm on overlapping triplet sets

$$\text{Alternation behavior}(\%) = \frac{\text{Actual alternations}}{\text{Possible alternations}} \times 100$$

Immunohistochemistry

Mice were immediately anesthetized after finishing behavioral tests and transcardially perfused with 0.05 mol/L PBS and ice-cold 4% paraformaldehyde in 0.1 mol/L phosphate buffer. Removed mouse brains were post-fixed in 4% paraformaldehyde in 0.1 mol/L phosphate buffer at 4°C for overnight and immersed in 30% solution of sucrose in 0.05 mol/L PBS. A freezing microtome (Leica Instruments GmbH, Nussloch, Germany) was utilized to obtain serial

coronal sections (30 μm thick) and, the sections were kept in cryoprotectant (25% ethylene glycol, 25% glycerol, and 0.05 mol/L phosphate buffer) at 4°C. For immunohistochemical assays, briefly rinsed brain sections were incubated with rabbit anti-neuronal nuclei (NeuN) (Merck Millipore, Darmstadt, Germany) at 4°C for overnight with normal goat serum and 0.3% Triton X-100. Then, the sections were reacted with anti-rabbit biotinylated IgG for 1 h, followed by incubation with ABC at room temperature for 1 h. After developing using DAB in 0.05 mol/L Tris-buffered saline (pH 7.6) to determine the peroxidase activity, histomount medium was added on gelatin-coated slides.

Chemicals and reagents

The AAL standard compounds (+)-catechin, chlorogenic acid, epicatechin, rutin, and isoquercitrin were provided by ChemFaces Biochemical Co., Ltd. (Wuhan, China); and kaempferol-3-O-rutinoside was obtained from Biopurify Phytochemicals (Chengdu, China). Purities of the chemicals were $\geq 98.0\%$. The high-performance liquid chromatography (HPLC)-grade solvents acetonitrile and water were purchased from J. T. Baker Chemical Co. (Phillipsburg, NJ). Trifluoroacetic acid (TFA) was purchased from Sigma-Aldrich (St Louis, MO).

Preparation of standard and sample solutions for HPLC analysis

For preparing sample solution, AAL extract was dissolved in 90% aqueous methanol (10 mg/mL of final concentration) and filtered using a syringe filter with 0.45 μm pore size. The stock solutions of six standard compounds were dissolved in methanol (1.0 mg/mL of final concentration). Working solutions of the standard compounds were prepared by diluting the stock solution to a final concentration of 0.1 mg/mL.

Chromatographic conditions

For HPLC analysis, Waters Alliance e2695 HPLC system (Waters Corp., Milford, MA) with a photodiode array (PDA) detector was used. Acquired data were processed using Empower software version 3. Chromatographic separation of the standard compounds was obtained using a Luna C18 analytical column (250 \times 4.6 mm, 5 μm ; Phenomenex, Torrance, CA) at 30°C. The mobile phases consisted of 0.1% (v/v) aqueous TFA (A) and acetonitrile (B). Conditions of the gradients were 10% B for 0–10 min, 10–50% B for 10–50 min, 50–100% B for 50–51 min, and 100% B for 51–60 min (injection volume: 10 μL , and flow rate: 1.0 mL/min). Ultraviolet (UV) wavelength of the PDA detector ranged from 190 to 400 nm.

Statistical analysis

Values were represented as mean \pm SEM. Statistical significance was analyzed using one-way analysis of variance and Dunnett's multiple comparisons test. Difference was considered if *P* value was less than 0.05.

Results

Effects of AAL extract on A β disaggregation and antioxidation

Amyloid deposition in the fibrillary aggregated form of A β is a crucial pathogenic mechanism underlying AD.¹⁶ To explore whether *A. atemoya* had inhibitory effects on A β aggregation, ethanol extracts from AAL, AAS, and AAF were prepared. At 100 $\mu\text{g}/\text{mL}$, AAL and AAF extracts increased the relative percentage of A β disaggregation by 91.35% and 38.92%, respectively. In contrast, AAS had no effect on A β disaggregation (Figure 1(a), left). As AAL extracts were the most effective at promoting A β disaggregation, we further explored its effect on A β aggregation at a broad range of concentrations. As shown in Figure 1(b) (left), AAL extract exerted a dose-dependent inhibition of A β aggregation.

Neurotoxic factors including A β in AD cause oxidative stress in the brain by perturbing the balance between oxidants and antioxidants.¹⁷ The scavenging activities of *A. atemoya* extracts against ABTS or DPPH were measured to examine antioxidant activities. Consistent with the results of the A β aggregation assay, ABTS and DPPH scavenging activity was exhibited by AAL, AAF, and AAS extracts (Figure 1(a), middle and right, respectively) in decreasing order. AAL extract dose-dependently enhanced scavenging activity against ABTS and DPPH radicals (Figure 1(b), middle and right, respectively).

We compared the effects of AAL extract with GB, LC, and AG extracts on inhibition of A β aggregation and activation of free radical scavenging. GB, LC, and AG are known medicinal plants that are effective on anti-AD.^{18–20}

As shown in Figure 1(c), AAL showed robust A β disaggregation activity compared with that of other extracts. Effects of AAL extract on antioxidation were similar to that of GB extract but higher than those of LC and AG extracts.

Neuroprotective effects of AAL extract on H₂O₂-damaged HT22 neuronal cells

Neuronal cell death is a major cause of neurodegenerative diseases including AD.^{21,22} To examine the effects of *A. atemoya* extracts on neuronal death, HT22 hippocampal cells were used. To determine the cytotoxicity of *A. atemoya* extracts, CCK assay, a sensitive colorimetric assay for the determination of cell viability in cytotoxicity assay, was performed. As shown in Figure 2(a), at concentrations up to 100 $\mu\text{g}/\text{mL}$, AAL and AAF extracts had no significant effect on cell viability. In contrast, AAS extract significantly reduced cell viability at 100 $\mu\text{g}/\text{mL}$ by 56.2% compared with that of untreated control.

Neuronal cell damage was mediated by exposing the cells to H₂O₂ (250 $\mu\text{mol}/\text{L}$), followed by the treatment with AAL, AAS, or AAF extracts at the range of non-toxic concentrations. The treatment with H₂O₂ alone significantly reduced the HT22 cell viability by 58.3% compared to untreated control. Of note, AAL extract significantly reversed H₂O₂-induced neuronal cell

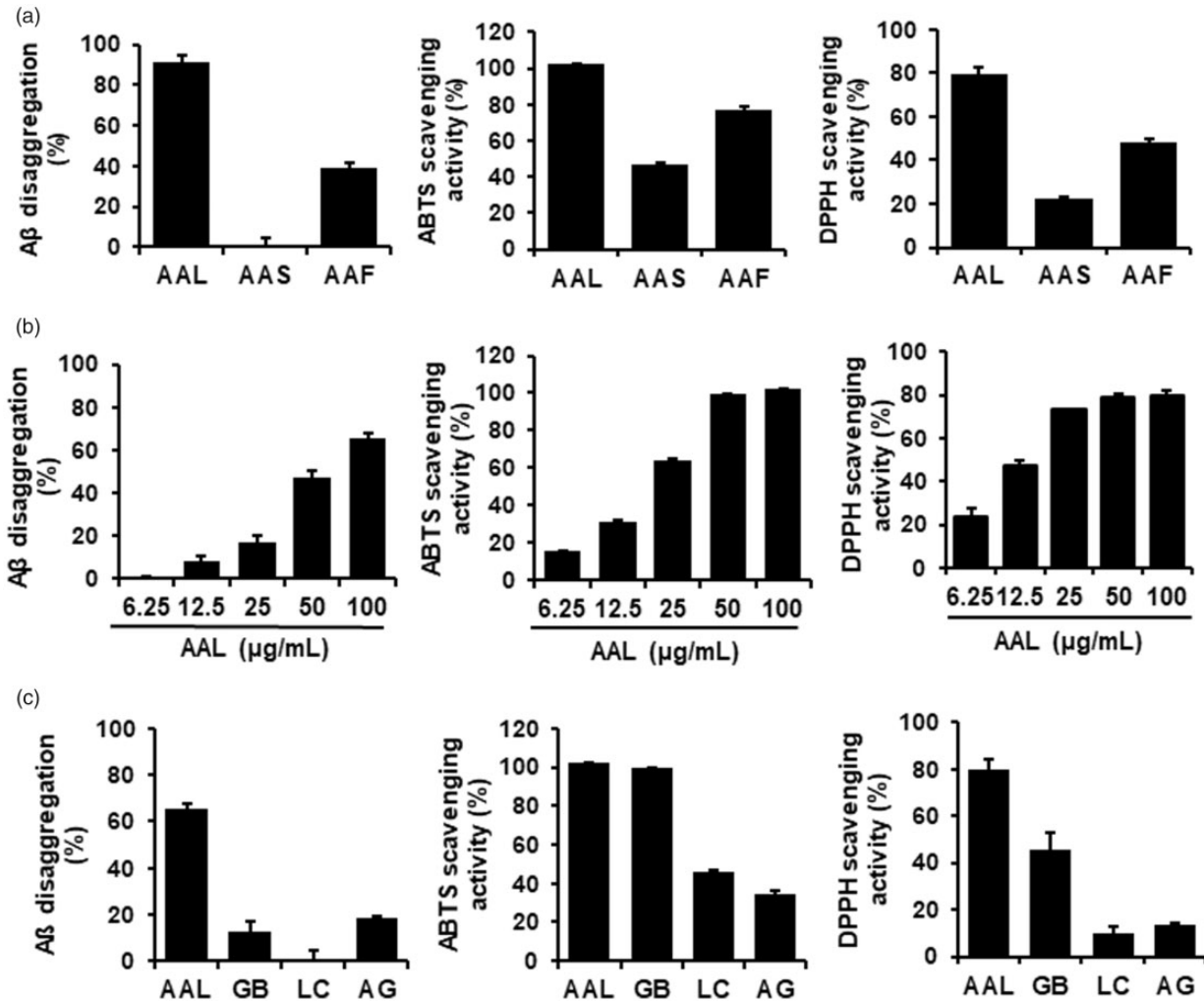


Figure 1. Effects of AAL extract on $A\beta$ aggregation and antioxidation. Assays were conducted by reaction with AAL, AAS, or AAF extracts at 100 $\mu\text{g/mL}$ (a); various concentrations (6.25, 12.5, 25, 50, or 100 $\mu\text{g/mL}$) of AAL extract (b); and AAL, GB, LC, or AG extract (c). (Left column) $A\beta$ aggregation assay was performed using the SensoLyte[®] Thioflavin T β -Amyloid aggregation kit. Samples were reacted with $A\beta$ (1–42) peptides, followed by the addition of Thioflavin T. Fluorescence of Thioflavin T was measured at an excitation wavelength of 440 nm and an emission wavelength of 485 nm. (Middle and right columns) Antioxidant activity was assessed by a free radical scavenging assay for ABTS (middle column) and DPPH (right column). Percent activity is equal to percent inhibition of ABTS and DPPH. Each value is presented as the mean \pm SEM ($n = 3$). AAL: *Annona atemoya* leaf, AAS: *A. atemoya* seed, AAF: *A. atemoya* fruit, GB: *Ginkgo biloba*, LC: *Lycium chinense*, and AG: *Angelica gigas*.

death at 25 or 50 $\mu\text{g/mL}$ (Figure 2(b)) whereas AAS and AAF extracts did not inhibit H_2O_2 -mediated cellular damage (Figure 2(c) and (d), respectively), indicating the neuroprotective effects of AAL, but not AAS or AAF. We further examined the neuroprotective effects of AAL by measuring the level of BDNF, a neuronal marker,²³ in H_2O_2 -treated HT22 cells. H_2O_2 treatment significantly reduced the amount of BDNF compared to that of untreated control. In contrast, AAL extract prevented the H_2O_2 -mediated inhibition of BDNF production at 50 $\mu\text{g/mL}$ when compared to that of treatment with H_2O_2 alone (Figure 2(e)).

Effects of BU fraction on $A\beta$ aggregation and neuroprotection

To determine which fraction of AAL extract exerted the greatest effects on $A\beta$ aggregation and neuroprotection, we prepared solvent fractions of HX, EA, BU, and H_2O

from AAL ethanol extracts. All tested fractions increased the inhibition of $A\beta$ aggregation in a dose-dependent manner. The inhibition percentages of HX, EA, BU, and H_2O at 100 $\mu\text{g/mL}$ were 34.9, 71.4, 90.2, and 66.0%, respectively (Figure 3(b) to (e)).

We tested the neuroprotective effects of each fraction of AAL extracts in H_2O_2 -treated HT22 cells. The cytotoxicity of the fractions was evaluated by CCK assay. Treatment with BU and H_2O fractions up to 100 $\mu\text{g/mL}$ had no significant effect on cell viability. In contrast, HX and EA fractions significantly decreased the cell viability in a dose-dependent manner (Figure 4(a)). Subsequent assays were performed using non-toxic concentrations.

As described above, neuronal cell damage was induced by adding H_2O_2 to HT22 cells. BU fraction significantly blocked H_2O_2 -induced damage of HT22 cells. All other fractions had no significant effect on cell damage (Figure 4(b) to (e)).

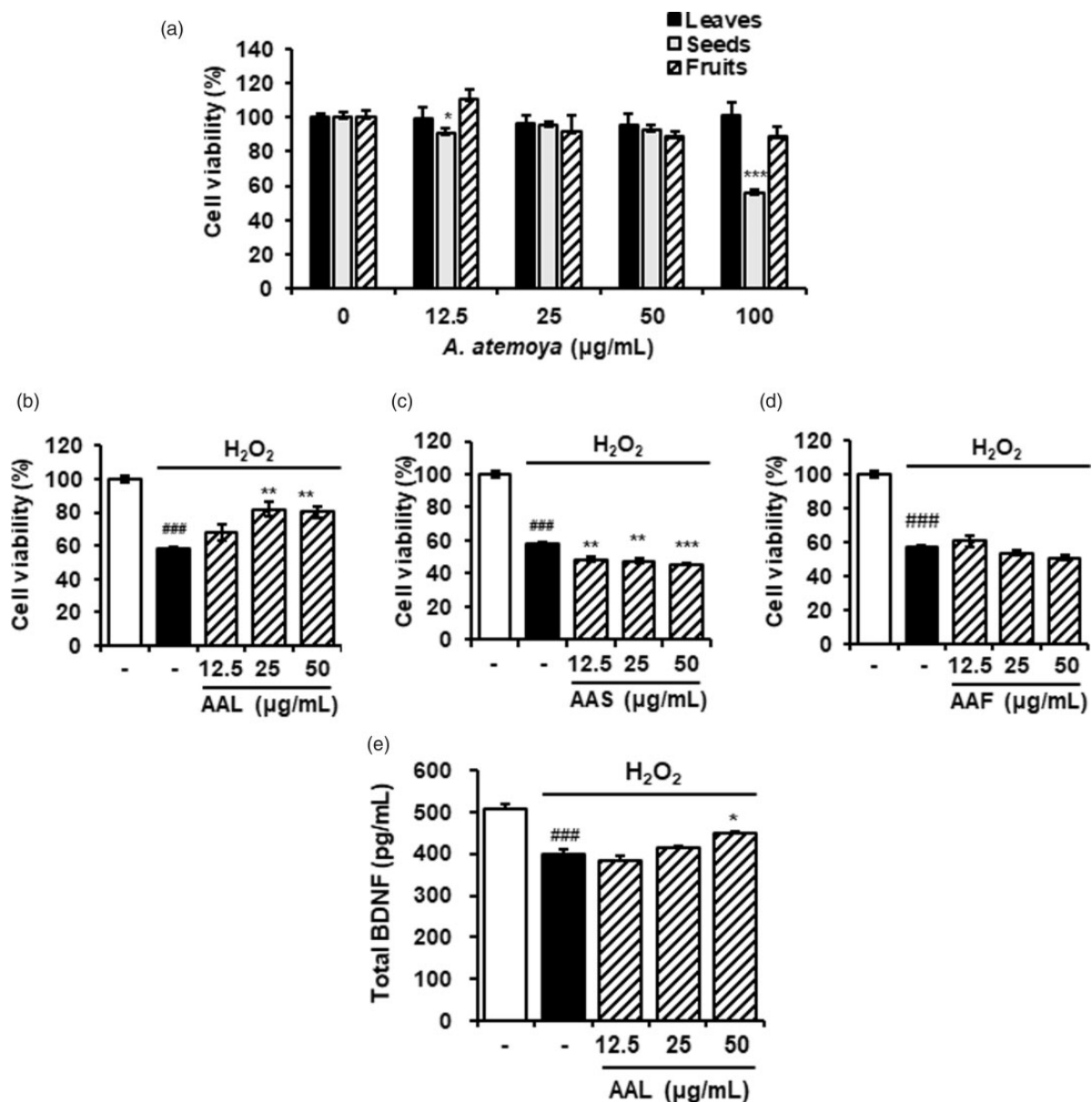


Figure 2. Neuroprotective effects of AAL extract in H_2O_2 -damaged HT22 cells. (a) Cytotoxicity of AAL, AAS, or AAF extracts was measured using the CCK assay against HT22 cells. The cells were treated with the extracts for 24 h. (b) Cells were exposed to H_2O_2 in the absence or presence of AAL, AAS, or AAF extracts for 6 h. Cell viability was determined using a CCK assay kit. (c) The production of BDNF was measured in the culture supernatant and assessed using ELISA. The results are expressed as mean \pm SEM of three independent experiments. ### $P < 0.001$ vs. vehicle control cells; * $P < 0.05$, ** $P < 0.01$, and *** $P < 0.001$ vs. H_2O_2 -treated cells. AAL: *Annona atemoya* leaf, AAS: *A. atemoya* seed, and AAF: *A. atemoya* fruit.

AAL extract ameliorates memory impairment in $\text{A}\beta$ -injected AD-like mice model

Memory loss is a main symptom of AD.²⁴ The effect of AAL extract on memory impairment induced by $\text{A}\beta$ was evaluated using the passive avoidance and Y-maze tests (Figure 5(a)). $\text{A}\beta$ aggregates were injected icv into male ICR mice to induce an AD-like mouse model. In the passive avoidance task, $\text{A}\beta$ aggregates significantly shortened the transfer latency compared to that of vehicle ($P < 0.01$). Administration of AAL extract at 100 mg/kg significantly increased transfer latency compared to that following $\text{A}\beta$ treatment ($P < 0.001$; Figure 5(b)). In the Y-maze test, AAL extract significantly reversed the spontaneous alternative

behavior of $\text{A}\beta$ -injected mice at 100 mg/kg (Figure 5(c)). Morin was used as a positive control.

Immunohistochemistry was performed against NeuN and BDNF in hippocampal tissues to elucidate the effects of AAL extract on neuronal marker expression. As shown in Figure 5(d) and (e), the decreased number of NeuN-positive cells was observed in the hippocampus of the $\text{A}\beta$ -administered group compared with the normal group. In contrast, AAL administration with $\text{A}\beta$ injection considerably reversed the effects of $\text{A}\beta$ treatment. Consistently, $\text{A}\beta$ injection reduced the immunoreactivity with anti-BDNF antibody whereas AAL administration inhibited $\text{A}\beta$ -mediated loss of BDNF expression in $\text{A}\beta$ -injected

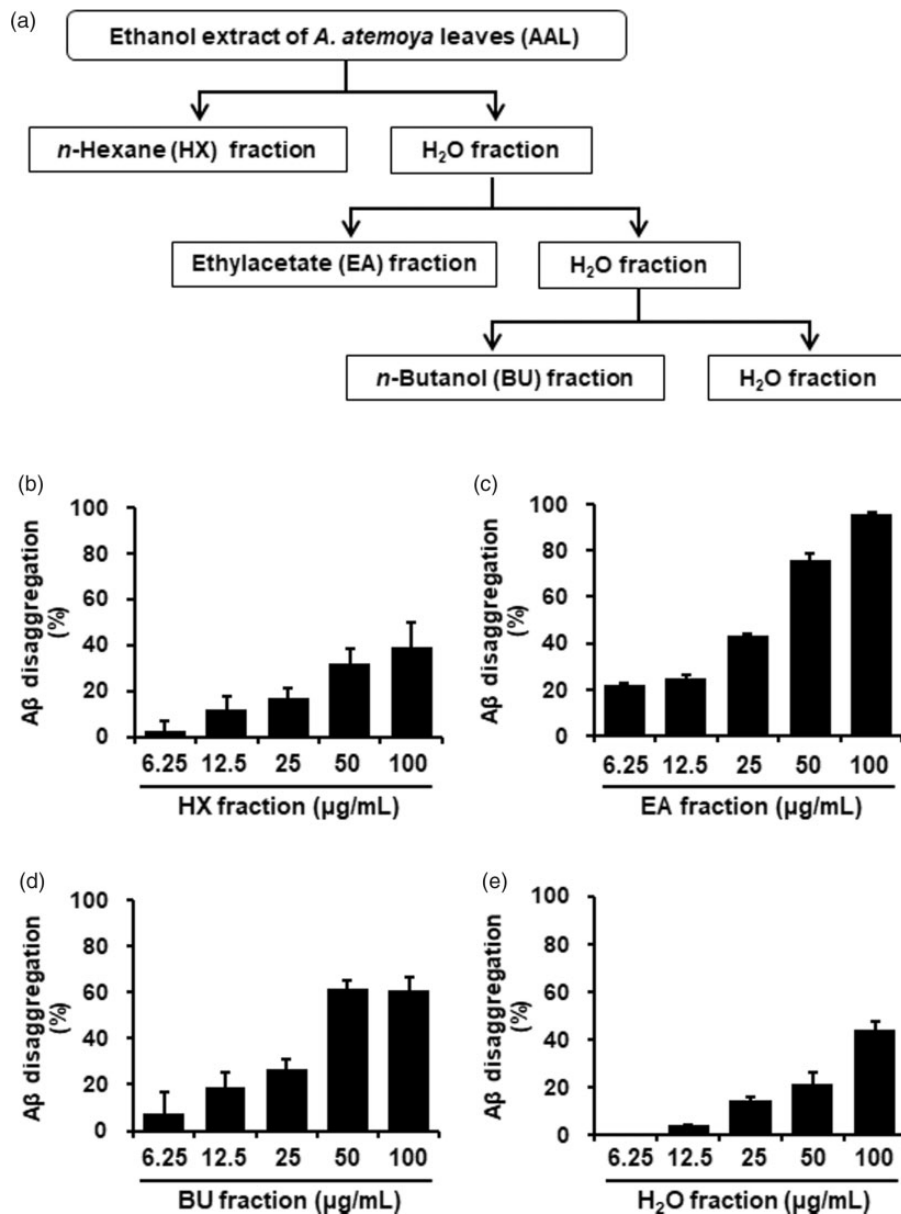


Figure 3. Effect of solvent fractions of AAL extract on A β aggregation and neuronal cell damage. (a) Flow diagram of fractionation of AAL extract. (b) A β aggregation assay was performed using the SensoLyte[®] Thioflavin T β -Amyloid aggregation kit. Various concentrations (6.25, 12.5, 25, 50, or 100 μ g/mL) of HX (b), EA (c), BU (d), and H₂O (e) fractions of AAL extract were reacted with A β (1–42) peptides, followed by the addition of Thioflavin T. Fluorescence of Thioflavin T was measured at an excitation wavelength of 440 nm and an emission wavelength of 485 nm. Each value is presented as the mean \pm SEM ($n = 3$). AAL: *Annona atemoya* leaf.

mouse. These data show the neuroprotective effect of AAL in a mouse model.

Molecular mechanisms underlying anti-AD effects of AAL extract

To investigate the regulatory mechanisms responsible for anti-AD effects of AAL, antibody microarray was performed using H₂O₂-treated HT22 cells with or without AAL extract. Of 1318 phospho-specific proteins, we observed that phosphorylation of four proteins (CaMK2 $\beta/\nu/\delta$, GRK2, EGFR, and Myc) was increased, and that of four proteins (FER, caveolin-1, NF κ B 65, and MLRL 2) was decreased by H₂O₂ treatment at specific tyrosine or serine residues (≥ 1.5 -fold change). Concurrent treatment with

AAL and H₂O₂ reversed phospho-levels of the proteins compared to that of treatment with H₂O₂ alone (Figure 6 (a)). Total protein quantification was used to normalize the phosphoprotein levels. Internal positive controls GAPDH and β -actin were constitutively expressed in all samples.

Western blotting was performed to validate the antibody microarray results using the anti-phospho-specific antibodies. AAL treatment reduced the phosphorylation of EGFR and GRK2 in H₂O₂-treated HT22 cells (Figure 6(b)). However, the results of Western blotting for other six phosphoproteins were not consistent with antibody microarray. The effect of AAL on phosphorylation of EGFR and GRK2 was confirmed in an AD-like mouse model. As shown in Figure 6(c), phosphorylation of EGFR and GRK2 was increased in A β -stimulated mouse tissue compared with

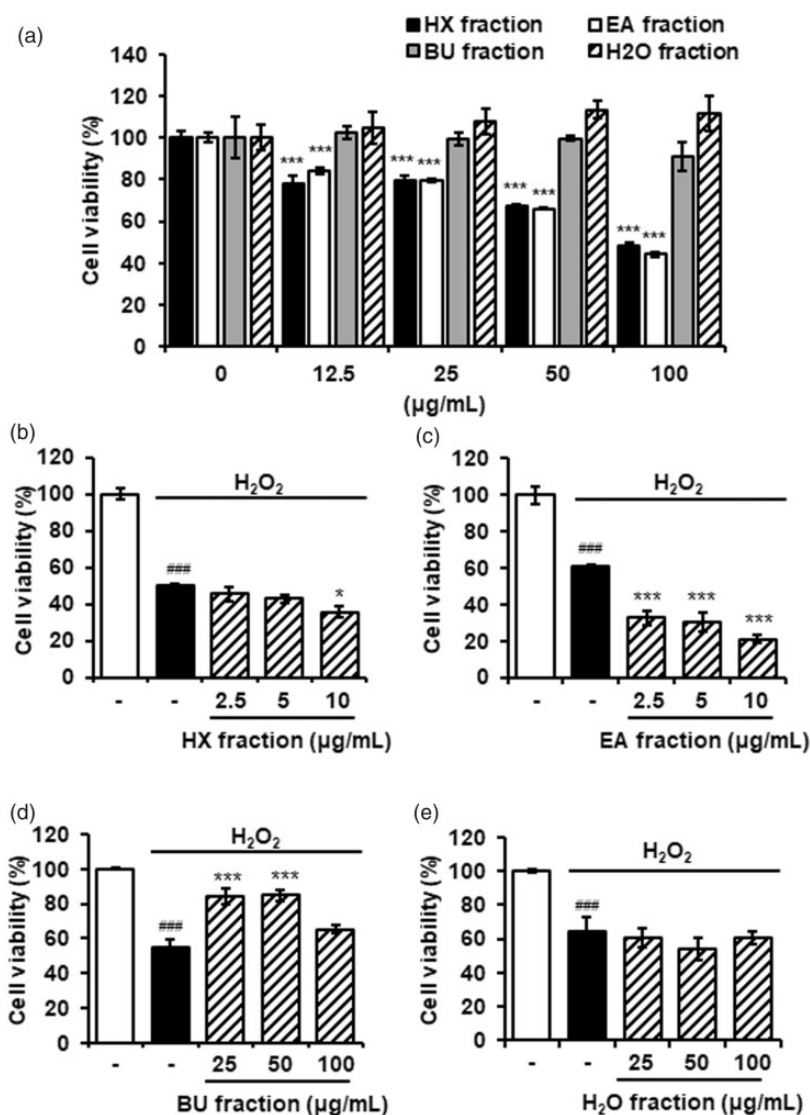


Figure 4. Neuroprotective effects of solvent fractions of AAL extract in H_2O_2 -damaged HT22 cells. (a) Cytotoxicity of *n*-hexane (HX), ethylacetate (EA), *n*-butanol (BU), and water (H_2O) fractions was measured using the CCK assay against HT22 cells. The cells were treated with the extracts for 24 h. The results are expressed as mean \pm SEM of three independent experiments. $***P < 0.001$ vs. untreated control cells. (b) to (e) HT22 cells were exposed to H_2O_2 in the absence or presence of HX (b), EA (c), BU (d), and H_2O (e) fractions for 6 h. Cell viability was determined using a CCK assay kit. The results are expressed as mean \pm SEM of three independent experiments. $###P < 0.001$ vs. vehicle control cells; $*P < 0.05$ or $***P < 0.001$ vs. H_2O_2 -treated cells. AAL: *Annona atemoya* leaf.

that of normal controls. In contrast, AAL administration reduced the $A\beta$ -mediated phosphorylation of EGFR and GRK2 compared with that of $A\beta$ administration alone.

HPLC determination of the six standard compounds in AAL

Optimized HPLC method was used for the simultaneous determination of the six standard compounds in AAL extract. The results showed well-separated chromatograms using mobile phases consisting of 0.1% (v/v) aqueous TFA (a) and acetonitrile (b). The UV wavelengths were 254 nm for rutin, isoquercitrin, and kaempferol-3-O-rutinoside, 280 nm for (+)-catechin and epicatechin, and 330 nm for chlorogenic acid. The six standard compounds were resolved within 27 min. The retention times for (+)-catechin, chlorogenic acid, epicatechin, rutin, isoquercitrin, and kaempferol-3-O-rutinoside were 11.39, 12.31,

17.8, 24.4, 25.45, and 26.73 min, respectively. HPLC chromatograms of AAL extract and standard compounds are shown in Figure 7.

Effect of standard compounds of AAL extract on the $A\beta$ disaggregation

To determine biologically active compound of AAL extract, we conducted the $A\beta$ aggregation assay using the AAL standard compounds. Among six compounds, isoquercitrin (Figure 8(a)) and rutin (Figure 8(b)) increased the ability of $A\beta$ disaggregation in a dose-dependent manner and reached 73.7% and 81.8% at 100 μ M, respectively. The maximum ratio of $A\beta$ disaggregation by (+)-catechin (Figure 8(c)), kaempferol-3-rutinoside (Figure 8(d)), epicatechin (Figure 8(e)) was less than 35%. Chlorogenic acid (Figure 8(f)) had no effect on the $A\beta$ disaggregation. Notably, we confirmed rutin and isoquercitrin were contained in BU

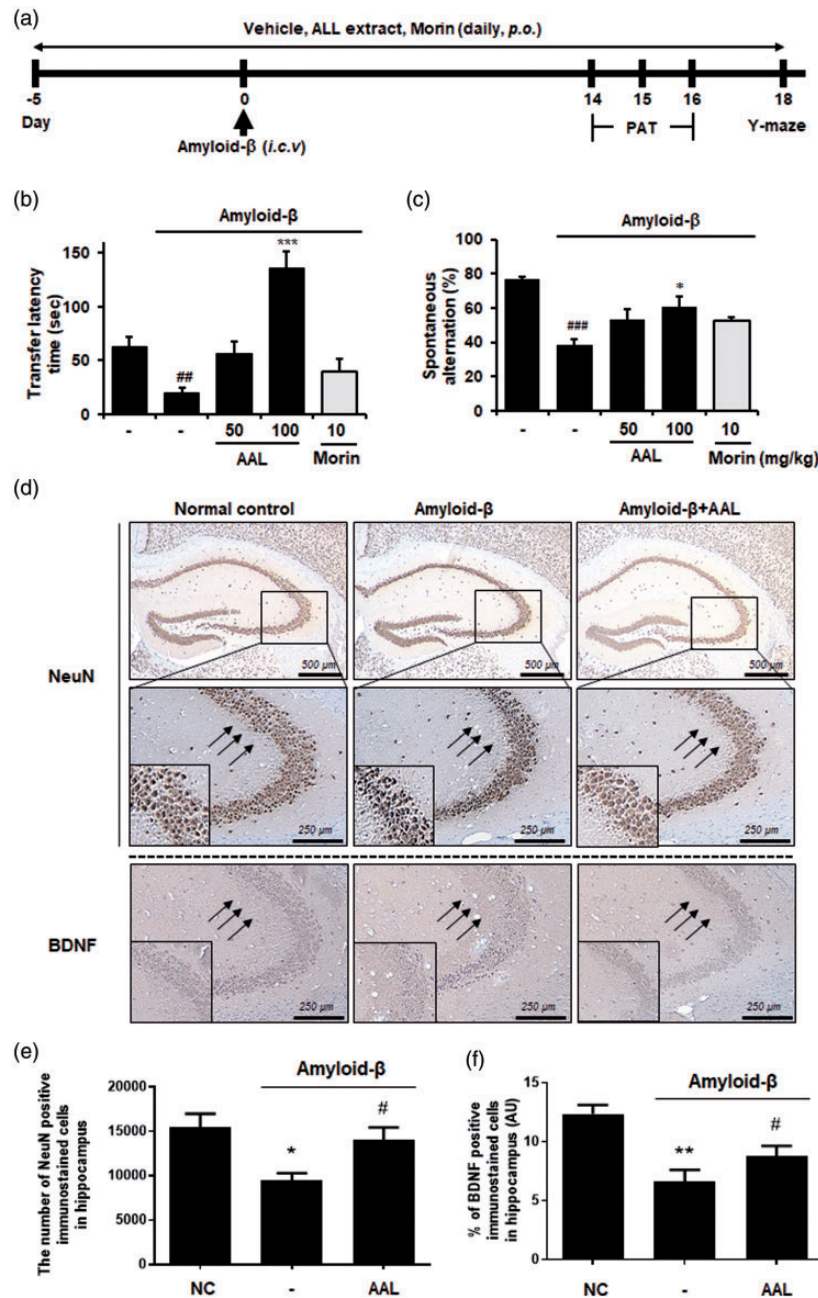


Figure 5. Effects of AAL extract on memory impairment in an A β -induced AD-like mouse model. (a) Time schedule of the animal experiments. (b) Male ICR mice were assigned to five groups ($n = 7/\text{group}$). A β aggregates (50 pmol per 10% DMSO in PBS) were injected into the intracerebroventricular region. Vehicle (saline), AAL (50 or 100 mg/kg), or morin (10 mg/kg) was orally administered for 23 days after adaptation for one week. (b) For the passive avoidance test, mice were trained on a one-trial step-through passive avoidance task on day 14 after A β injection (retention trial). The testing trial was given two days after the training trial (acquisition trial). The latency time was recorded at the retention and acquisition trials. (c) Y-maze was performed on day 18 after A β injection. Spontaneous alternation behavior was measured during an 8-min session. The data are presented as means \pm SEM. ^{##} $P < 0.01$ vs. normal group. ^{*} $P < 0.05$, and ^{***} $P < 0.001$ vs. A β control group. Morin was used as a positive control for inhibitor of A β aggregation. (d) Expression of NeuN and BDNF in hippocampus was determined by immunohistochemistry (magnification $\times 200$). (e) Quantification of the BDNF positive stained cell density within the hippocampus (proportion of BDNF positive staining over the hippocampus area) was compared between experimental groups (section from $n = 3$ brains were analyzed per group). (f) The number of neurons in different areas of the brain was estimated by automated cell counting (particle analysis) using the Image J software. NC: normal control, AAL: *Annona atemoya* leaf. (A color version of this figure is available in the online journal.)

layer, an active fraction of AAL extract, using HPLC analysis (Figure 8(g)).

Discussion

Natural products are naturally occurring substances that include phytochemicals and herbal medicines.²⁵

Accumulating evidences demonstrate the powerful antioxidant activity of many natural products.^{26–28} An optimal level of reactive oxygen species (ROS) is essential for regulation of cellular processes. However, excessive ROS generation is harmful to biomolecules and induces oxidative stress in various chronic diseases.²⁹ Therefore, elevating antioxidant activity by activating antioxidant enzymes

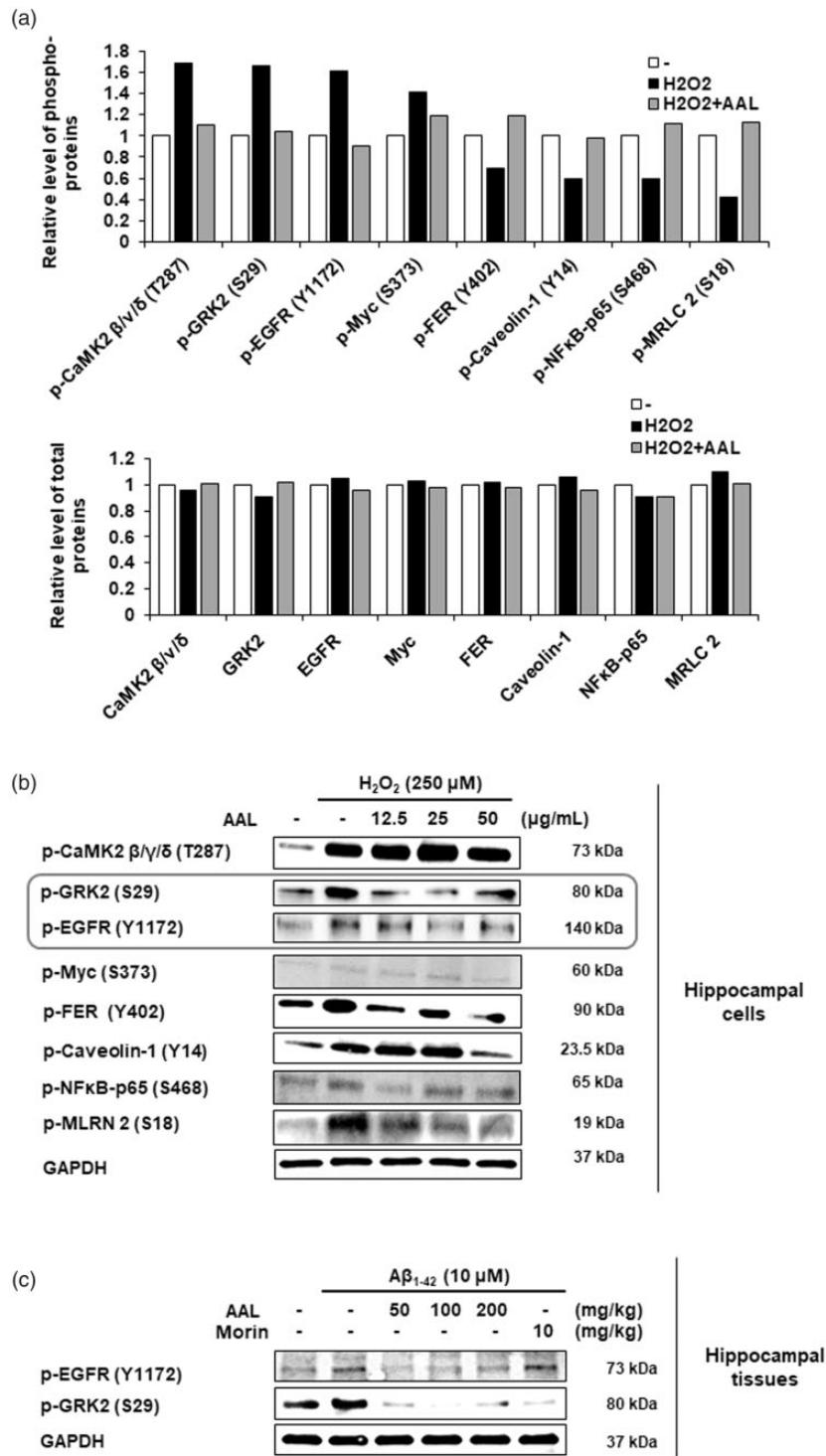


Figure 6. Molecular mechanisms responsible for anti-AD effects of AAL extract. (a) HT22 cells were exposed to H₂O₂ in the absence or presence of AAL extract (50 μg/mL) for 6 h. Antibody microarray assay was performed using the phospho-specific antibody microarray slide (Full Moon BioSystems). For data acquisition, GenePix 4100A scanner (Axon Instrument, USA) was used. The normalization data were analyzed using Genowiz 4.0™ (Ocimum Biosolutions). The phosphorylation ratio was calculated and represented as fold changes of indicated phosphoproteins after H₂O₂ treatment normalized to total protein expression (upper panel). Total protein quantification is shown (lower panel). (b) HT22 cells were exposed to H₂O₂ with or without various concentrations of AAL extract (0, 12.5, 25, or 50 μg/mL) for 6 h. Cell lysates were prepared from HT22 cells and equal amounts of protein were subjected to Western blotting using anti-phospho-CaMK2 β/γ/δ, GRK2, EGFR, Myc, FER, caveolin-1, NFκB p65, and MLRN 2 antibodies to validate the Ab microarray. (c) Protein extracts were prepared from hippocampal tissues in an Aβ-induced AD mouse model. Vehicle or various concentrations of AAL extract (50, 100, or 200 mg/kg) were administered to Aβ mice for 23 days. Western blotting was performed for anti-phospho-EGFR and phospho-GRK2. The validity of the two phospho-antibodies was determined using pre-stained protein marker (Bio-Rad). GAPDH was used as an internal control. Shown blots are representative results from three independent experiments.

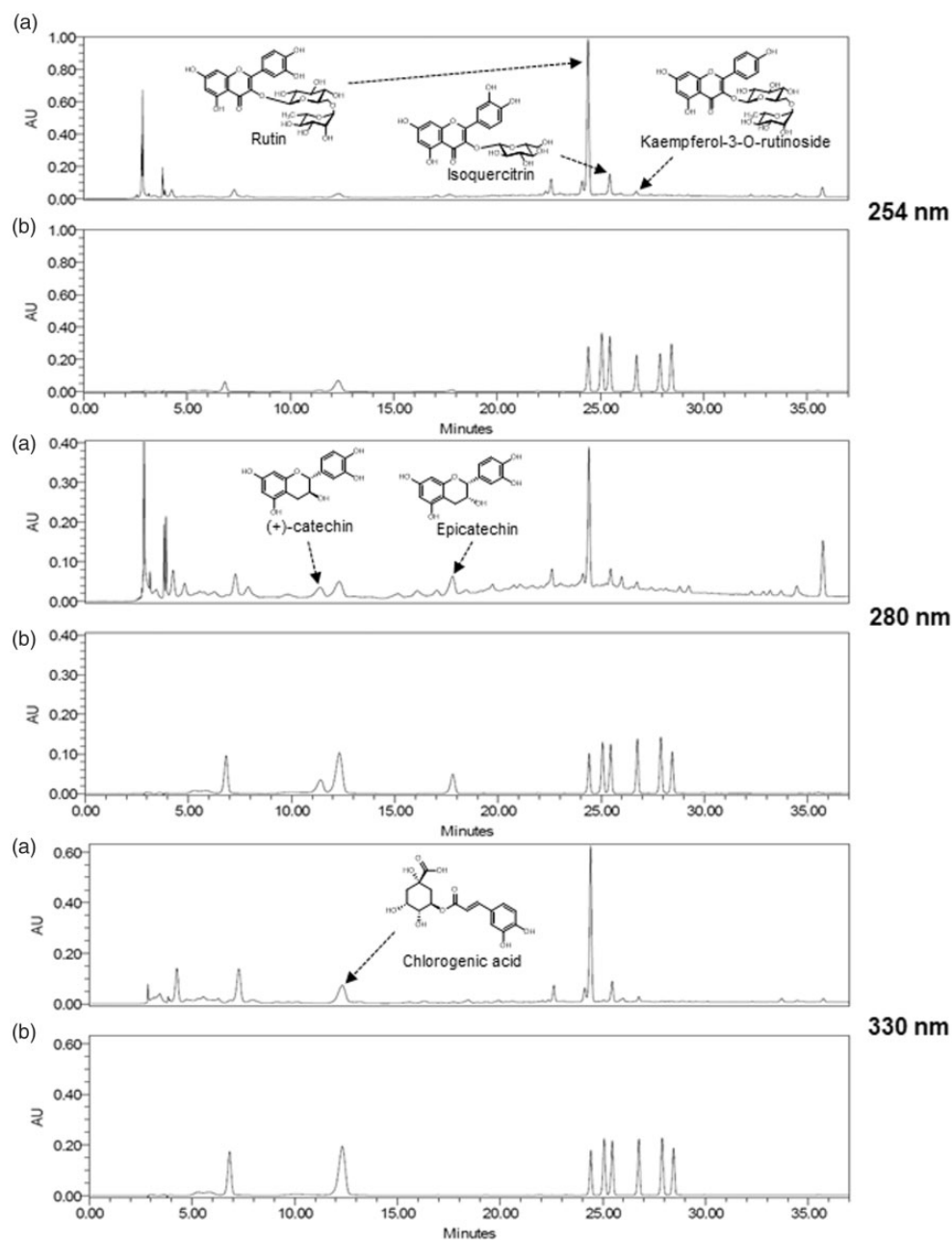


Figure 7. HPLC chromatograms of the ethanol extract of AAL (a) and standard mixture (b) at 254, 280, and 330 nm.

and free radical scavenging rates may be a beneficial therapeutic approach for chronic diseases.⁵ In this regard, natural products are attractive materials for drug discovery and as functional foods. In addition, most natural products have lower toxicity and less side effects compared to those of synthetic drugs.^{30,31}

Our study explored the efficacy of AAL using neuronal cells and an AD-like mouse model. *A. atemoya* grows and is marketed in subtropical and tropical areas. AAF is generally harvested in fall and winter depending on the region; leaf-dropping occurs from fall to spring.^{6,7} AAF is eaten raw or utilized for juice, ice cream, desserts, and liquors.⁷ Unlike AAF, there are no reports on the usage and biological effects of AAL. Here, we report that AAL extract has the therapeutic potential for AD or AD-related diseases.

Our data revealed that AAL extract inhibited A β aggregation, the hallmark of AD pathology,¹⁶ and enhanced anti-oxidant activity compared to that of AAF and AAS extracts. In addition, we observed that AAL extract possessed greater potential than that of other medicinal plants such as GB, LC, and AG that have previously been reported to have anti-AD effects.^{18–20}

To date, five drugs were approved by the US Food and Drug Administration for AD. Unfortunately, the drugs do not act as therapeutics for AD. They delay the progression or provide relief of symptoms, but are accompanied by adverse effects such as muscle cramps, bradycardia, and gastrointestinal disorders. The drugs are AChE inhibitors (donepezil, tacrine, galantamine, and rivastigmine) or NMDA receptor antagonists (memantine).^{1,2}

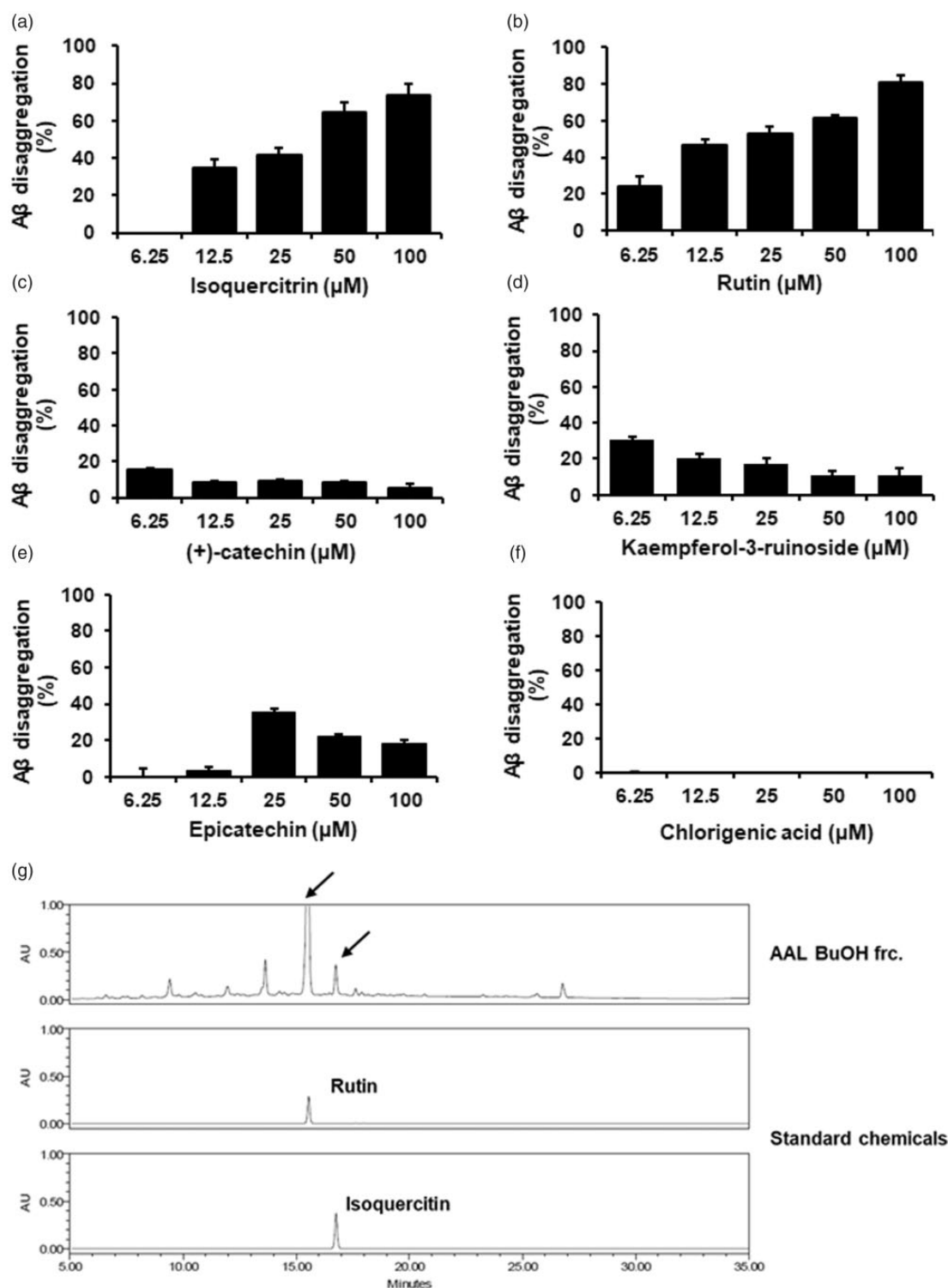


Figure 8. Effect of standard compounds of AAL extract on the A β disaggregation. A β aggregation assay was performed using the Sensolyte[®] Thioflavin T β -Amyloid aggregation kit. Various concentrations (6.25, 12.5, 25, 50 or 100 μ mol/L) of AAL standard compounds isoquercitrin (a), rutin (b), (+)-catechin (c), kaempferol-3-rutinoside (d), epicatechin (e), and chlorogenic acid (f) were reacted with A β (1–42) peptides, followed by the addition of Thioflavin T. Fluorescence of Thioflavin T was measured at an excitation wavelength of 440 nm and an emission wavelength of 485 nm. Each value is presented as the mean \pm SEM ($n = 3$). (g) HPLC chromatogram of BU fraction from AAL extract at 245 nm. Rutin and isoquercitrin were used as standard compounds.

Thus, new drug targets have been sought as drugs to treat AD. Recent studies have explored drugs that inhibit A β aggregation as a potential therapeutic for AD. Abnormal A β accumulation in the brains of AD patients is significantly associated with oxidative damage.^{5,32} The oxidative

stress in AD brains is caused by the imbalance between oxidants and antioxidants due to over-production of free radicals.⁵ As mentioned above, natural products such as herbal medicines have robust antioxidant capacity. AAL extract dramatically enhanced the scavenging rates against

ABTS and DPPH, indicating antioxidant activity of AAL. Excess concentration of A β acts as a neurotoxin thereby inducing neuronal cell death and oxidative stress.³³ We thus investigated whether AAL extract had neuroprotective effects using HT22 mouse hippocampal cells. We and others have used H₂O₂-treated HT22 cells in AD studies.^{34–36} AAL extract, but not AAF or AAS, significantly prevented H₂O₂-induced neuronal cell death. Our findings suggest that AAL extract has protective effects in neuronal cells damaged by oxidative stress.

Memory loss associated with aging is known as age-related memory impairment.³⁷ Memory impairment is a main symptom in the pathogenesis of AD and AD-related diseases, that are controlled by different brain mechanisms.²¹ Several AD-related animal models involving genetically and/or non-genetically engineered animals have been established, and their pathophysiological characteristics have been identified. Recently, we reported that A β -injected mice, 5xFAD mice, and initial phase bilateral common carotid artery occlusion rats have similar molecular features compared to those of human AD patients, supporting their validity as models for AD.³⁸ In the present study, we utilized an A β -injected AD-like mouse model. AAL extract was orally administered for 23 days, and behavioral tests were conducted. AAL administration displayed a significant preventive effect on memory impairment induced by A β aggregates in the passive avoidance task and Y-maze test. The effects of AAL at 100 mg/kg/day were greater than those of morin, a positive control for A β inhibition.³⁹

The hippocampus plays an important role in learning and memory by interplaying with the prefrontal cortex.⁴⁰ In AD and other dementia patients, the hippocampus is the first brain region to suffer from oxidative stress and related damage.⁴¹ Neuronal markers NeuN and BDNF are altered in the hippocampi of AD-like mice model.^{42,43} In our immunohistochemical analysis, A β treatment suppressed the expression of neuronal markers NeuN and BDNF in hippocampal tissues. AAL reversed the effect of A β on NeuN and BDNF expression. Taken together, our results provide evidence for anti-AD activity of AAL via inhibition of A β aggregation, antioxidation, neuronal cell protection, and prevention of memory impairment.

To expand our investigations into the molecular mechanisms underpinning anti-AD effects of AAL, we performed a phosphoprotein antibody microarray consisting of >1000 phospho-antibodies from >30 signaling pathways. In HT22 hippocampal cells, H₂O₂ stimulation increased the phosphorylation of EGFR and GRK2 among the phosphoproteins tested, while AAL treatment in H₂O₂-stimulated cells showed similar levels of phospho-EGFR and GRK2 compared with those of untreated control. Antibody microarray results were validated by immunoblotting *in vitro* and *in vivo*. Consistently, AAL extract blocked the phosphorylation of EGFR and GRK2 in H₂O₂-damaged neuronal cells and hippocampal tissues from A β -injected mice. EGFR is a transmembrane protein that plays pivotal roles in cell proliferation and differentiation.⁴⁴ EGFR signaling in the brain is important in central nervous system development.⁴⁵ GRK2, also known as β -ARK (beta adrenergic receptor

kinase), is a serine/threonine intracellular kinase. Activation of EGFR stimulates GRK2 activity.⁴⁶ In relation to the study of AD, neuronal EGFR signaling is associated with presenilin 1, the most common cause of familial AD, in the regulation of neuroprotection in AD patients.⁴⁷ Several studies reported dysfunction of GRK2 in AD, especially at early stages.^{48–50} However, the association of EGFR and GRK2 in AD has yet to be identified. Further investigations are required to elucidate the roles of EGFR/GRK2 and their related signaling factors in AD pathogenesis at both protein and gene levels.

We finally determined the biologically active compound of AAL to regulate anti-AD effect. Among the six standard compounds (five flavonoids: (+)-catechin, epicatechin, rutin, isoquercitrin, and kaempferol-3-O-rutinoside, one phenolic acid: chlorogenic acid), isoquercitrin and rutin markedly increased inhibitory activity on the A β aggregation in a dose-dependent manner. We also identified that both isoquercitrin and rutin were included in BU fraction, an active fraction of AAL extract. Considering biological activity and the content of compound, rutin maybe the active compound of AAL.

Conclusions

Overall, it is of note that we demonstrate the biological activity of AAL for the first time. AAL extract strikingly prevented A β aggregation and attenuated memory impairment through inhibition of the EGFR/GRK2 phosphorylation *in vitro* and *in vivo*. Rutin was identified as an active compound of AAL to regulate anti-AD activity. Our findings demonstrate that AAL has potential as a therapeutic drug candidate for AD or AD-related disorders as well as functional food for improving cognitive or memory impairment.

Authors' contributions: H-SL and S-JJ conceived and designed the experiments. H-SL, ES, and S-JJ conducted the cell experiments. H-SL, YJK, ES, and S-JJ assisted with the animal experiments. H-SL, B-YK, and S-JJ analyzed the data and performed the statistical analysis. YJK conducted AAL extract and analysis using HPLC. H-SL and S-JJ wrote and helped to modify the paper. All authors read and approved the final version of the manuscript.

ACKNOWLEDGMENTS

We thank Drs Chang-Seob Seo and Mee-Young Lee in Korea Institute of Oriental Medicine for kind donation of plant materials.

DECLARATION OF CONFLICTING INTERESTS

The author(s) declared no potential conflicts of interest with respect to the research, authorship, and/or publication of this article.

FUNDING

The author(s) disclosed receipt of the following financial support for the research, authorship, and/or publication of

this article: This study was supported by a research grant (KSN1515293) from the Korea Institute of Oriental Medicine (KIOM).

ORCID iD

Soo-Jin Jeong  <https://orcid.org/0000-0001-6529-1767>

REFERENCES

1. Yiannopoulou KG, Papageorgiou SG. Current and future treatments for Alzheimer's disease. *Ther Adv Neurol Disord* 2013;**6**:19-33
2. Birks J. Cholinesterase inhibitors for Alzheimer's disease. *Cochrane Database Syst Rev* 2006;**25**:Cd005593
3. Teich AF, Arancio O. Is the amyloid hypothesis of Alzheimer's disease therapeutically relevant?. *Biochem J* 2012;**446**:165-77
4. Sadigh-Eteghad S, Sabermarouf B, Majidi A, Talebi M, Farhoudi M, Mahmoudi J. Amyloid-beta: a crucial factor in Alzheimer's disease. *Med Princ Pract* 2015;**24**:1-10
5. Huang WJ, Zhang X, Chen WW. Role of oxidative stress in Alzheimer's disease. *Biomed Rep* 2016;**4**:519-22
6. Crane JH, Balerdi CF, Orfanedes MS. Tropical and subtropical fruit crops for the home landscape: Alternatives to citrus. *UF IFAS Extension* 2010;**812**:1-8
7. Brandão AE, Santos DY. *National composition of fruit cultivars*. San Diego, CA: Academic Press, 2016, pp.195-214
8. Paull RE, Duarte O. Tropical fruits. *Crop Prod Sci Horticulture* 2011;**1**:148-50
9. Chih HW, Chiu HF, Tang KS, Chang FR, Wu YC. Bullatacin, a potent antitumor annonaceous acetogenin, inhibits proliferation of human hepatocarcinoma cell line 2.2.15 by apoptosis induction. *Life Sci* 2001;**69**:1321-31
10. Chiu HF, Chih TT, Hsian YM, Tseng CH, Wu MJ, Wu YC. Bullatacin, a potent antitumor annonaceous acetogenin, induces apoptosis through a reduction of intracellular cAMP and cGMP levels in human hepatoma 2.2.15 cells. *Biochem. Pharmacol* 2003;**65**:319-27
11. Yi JM, Park JS, Lee J, Hong JT, Bang OS, Kim NS. Anti-angiogenic potential of an ethanol extract of *Annona atemoya* seeds in vitro and in vivo. *BMC Complement Altern Med* 2014;**14**:353
12. Lim HS, Kim YJ, Sohn E, Yoon J, Kim BY, Jeong SJ. Bojungkigi-Tang, a traditional herbal formula, exerts neuroprotective effects and ameliorates memory impairments in Alzheimer's disease-like experimental models. *Nutrients* 2018;**10**:E1952
13. Re R, Pellegrini N, Proteggente A, Pannala A, Yang M, Rice-Evans C. Antioxidant activity applying an improved ABTS radical cation decolorization assay. *Free Radic Bio Med* 1999;**26**:1231-7
14. Moreno MI, Isla MI, Sampietro AR, Vattuone MA. Comparison of the free radical-scavenging activity of propolis from several regions of Argentina. *J Ethnopharmacol* 2000;**71**:109-14
15. Lim HS, Kim BY, Kim YJ, Jeong SJ. Phytochemical allylguaiacol exerts a neuroprotective effect on hippocampal cells and ameliorates scopolamine-induced memory impairment in mice. *Behav Brain Res* 2018;**339**:261-8
16. Murphy MP, LeVine H 3rd. Alzheimer's disease and the amyloid-beta peptide. *J Alzheimer's Dis* 2010;**19**:311-23
17. Liu Z, Zhou T, Ziegler AC, Dimitrion P, Zuo L. Oxidative stress in neurodegenerative diseases: from molecular mechanisms to clinical applications. *Oxid Med Cell Longev* 2017;**2017**:2525967
18. Rapp M, Burkart M, Kohlmann T, Bohlken J. Similar treatment outcomes with *Ginkgo biloba* extract EGb 761 and donepezil in Alzheimer's dementia in very old age: a retrospective observational study. *Int J Clin Pharmacol Ther* 2018;**56**:130-3
19. Ye M, Moon J, Yang J, Hwa Lim H, Bin Hong S, Shim I, Bae H. The standardized *Lycium chinense* fruit extract protects against Alzheimer's disease in 3xTg-AD mice. *J Ethnopharmacol* 2015;**172**:85-90
20. Li L, Li W, Jung SW, Lee YW, Kim YH. Protective effects of decursin and decursinol angelate against amyloid beta-protein-induced oxidative stress in the PC12 cell line: the role of Nrf2 and antioxidant enzymes. *Biosci Biotechnol Biochem* 2011;**75**:434-42
21. Gorman AM. Neuronal cell death in neurodegenerative diseases: recurring themes around protein handling. *J Cell Mol Med* 2008;**12**:2263-80
22. Hroudova J, Singh N, Fisar Z. Mitochondrial dysfunctions in neurodegenerative diseases: relevance to Alzheimer's disease. *Biomed Res Int* 2014;**2014**:175062
23. Silva A, Pereira J, Oliveira CR, Relvas JB, Rego AC. BDNF and extracellular matrix regulate differentiation of mice neurosphere-derived cells into a GABAergic neuronal phenotype. *J Neurosci Res* 2009;**87**:1986-96
24. Jahn H. Memory loss in Alzheimer's disease. *Dialogues Clin Neurosci* 2013;**15**:445-54
25. Editorial. All natural. *Nat Chem Biol* 2007;**3**:351
26. Nogueira CC, Paixao IC, Teixeira VL. Antioxidant activity of natural products isolated from red seaweeds. *Nat Prod Commun* 2014;**9**:1031-6
27. Ribeiro D, Freitas M, Silva AMS, Carvalho F, Fernandes E. Antioxidant and pro-oxidant activities of carotenoids and their oxidation products. *Food Chem Toxicol* 2018;**120**:681-99
28. Sharmin T, Rahman MS, Mohammadi H. Investigation of biological activities of the flowers of *Lagerstroemia speciosa*, the jarul flower of Bangladesh. *BMC Complement Altern Med* 2018;**18**:231
29. Alfadda AA, Sallam RM. Reactive oxygen species in health and disease. *J Biomed Biotechnol* 2012;**2012**:936486
30. Harvey AL. Natural products in drug discovery. *Drug Discov Today* 2008;**13**:894-901
31. Yuan H, Ma Q, Ye L, Piao G. The traditional medicine and modern medicine from natural products. *Molecules* 2016;**21**:E559
32. Christen Y. Oxidative stress and Alzheimer' disease. *Am J Clin Nutr* 2000;**71**:621S-9S
33. Cheignon C, Tomas M, Bonnefont-Rousselot D, Faller P, Hureau C, Collin F. Oxidative stress and the amyloid beta peptide in Alzheimer's disease. *Redox Biol* 2018;**14**:450-64
34. Martínez E, Navarro A, Ordóñez C, Del Valle E, Tolivia J. Oxidative stress induces apolipoprotein D overexpression in hippocampus during aging and Alzheimer's disease. *J Alzheimers Dis* 2013;**6**:129-44
35. Chao X, He X, Yang Y, Zhou X, Jin M, Liu S, Cheng Z, Liu P, Wang Y, Yu J, Tan Y, Huang Y, Qin J, Rapposelli S, Pi R. Design, synthesis and pharmacological evaluation of novel tacrine-caffeic acid hybrids as multi-targeted compounds against Alzheimer's disease. *Bioorg Med Chem Lett* 2012;**22**:6498-502
36. Lim HS, Kim YJ, Sohn E, Yoon J, Kim BY, Jeong SJ. Bojungkigi-Tang, a traditional herbal formula, exerts neuroprotective effects and ameliorates memory impairments in Alzheimer's disease-like experimental models. *Nutrients* 2018;**10**:1952
37. Hedden T, Gabrieli JD. Insights into the ageing mind: a view from cognitive neuroscience. *Nat Rev Neurosci* 2004;**5**:87-96
38. Kim BY, Lim HS, Kim Y, Kim YJ, Koo I, Jeong SJ. Evaluation of animal models by comparison with human late-onset Alzheimer's disease. *Mol Neurobiol* 2018;**55**:9234-50
39. Lemkul JA, Bevan DR. Morin inhibits the early stages of amyloid beta-peptide aggregation by altering tertiary and quaternary interactions to produce "off-pathway" structures. *Biochemistry* 2012;**51**:5990-6009
40. Preston AR, Eichenbaum H. Interplay of hippocampus and prefrontal cortex in memory. *Curr Biol* 2013;**23**:R764-773
41. Anand KS, Dhikav V. Hippocampus in health and disease: an overview. *Ann Indian Acad Neurol* 2012;**15**:239-46
42. Choi M, Lee Y, Cho SH. *Angelica tenuissima* Nakai ameliorates cognitive impairment and promotes neurogenesis in mouse model of Alzheimer's disease. *Chin J Integr Med* 2018;**24**:378-84
43. Hsiao YH, Hung HC, Chen SH, Gean PW. Social interaction rescues memory deficit in an animal model of Alzheimer's disease by increasing BDNF-dependent hippocampal neurogenesis. *J Neurosci* 2014;**34**:16207-19
44. Wee P, Wang Z. Epidermal growth factor receptor cell proliferation signaling pathways. *Cancers* 2017;**9**:E52
45. Rahn T, Leippe M, Roeder T, Fedders H. EGFR signaling in the brain is necessary for olfactory learning in *drosophila* larvae. *Learn Mem* 2013;**20**:194-200

46. Chen Y, Long H, Wu Z, Jiang X, Ma L. EGF transregulates opioid receptors through EGFR-mediated GRK2 phosphorylation and activation. *Mol Biol Cell* 2008;**19**:2973–83
47. Bruban J, Voloudakis G, Huang Q, Kajiwara Y, Al Rahim M, Yoon Y, Shioi J, Gama Sosa MA, Shao Z, Georgakopoulos A, Robakis NK. Presenilin 1 is necessary for neuronal, but not glial, EGFR expression and neuroprotection via gamma-secretase-independent transcriptional mechanisms. *FASEB J* 2015;**29**:3702–12
48. Obrenovich ME, Palacios HH, Gasimov E, Leszek J, Aliev G. The GRK2 overexpression is a primary hallmark of mitochondrial lesions during early Alzheimer disease. *Cardiovasc Psychiatry Neurol* 2009;**2009**:327360
49. Obrenovich ME, Smith MA, Siedlak SL, Chen SG, de la Torre JC, Perry G, Aliev G. Overexpression of GRK2 in Alzheimer disease and in a chronic hypoperfusion rat model is an early marker of brain mitochondrial lesions. *Neurotox Res* 2006;**10**:43–56
50. Suo Z, Wu M, Citron BA, Wong GT, Festoff BW. Abnormality of G-protein-coupled receptor kinases at prodromal and early stages of Alzheimer's disease: an association with early beta-amyloid accumulation. *J Neurosci* 2004;**24**:3444–52

(Received July 10, 2019, Accepted October 8, 2019)